

1 COVID-19 pandemic dynamics in India, the SARS-CoV-2 Delta variant, 2 and implications for vaccination

3 Wan Yang^{1*} and Jeffrey Shaman²

4 ¹Department of Epidemiology, ²Department of Environmental Health Sciences, Mailman School
5 of Public Health, Columbia University, New York, NY, USA

6 *Correspondence to: wy2202@cumc.columbia.edu

7 8 **Abstract**

9 **Background:** The COVID-19 Delta pandemic wave in India surged and declined within 3
10 months; cases then remained low despite the continued spread of Delta elsewhere. Here we
11 aim to estimate key epidemiological characteristics of the Delta variant based on data from
12 India and examine the underpinnings of its dynamics.

13
14 **Methods:** We utilize multiple datasets and model-inference methods to reconstruct COVID-19
15 pandemic dynamics in India during March 2020 – June 2021. We further use model estimates to
16 retrospectively predict cases and deaths during July – mid-Oct 2021, under various vaccination
17 and vaccine effectiveness (VE) settings to estimate the impact of vaccination and VE for non-
18 Delta-infection recoverees.

19
20 **Findings:** We estimate that Delta escaped immunity in 34.6% (95% CI: 0 – 64.2%) of individuals
21 with prior wildtype infection and was 57.0% (95% CI: 37.9 – 75.6%) more infectious than
22 wildtype SARS-CoV-2. Models assuming higher VE among those with prior non-Delta infection,
23 particularly after the 1st dose, generated more accurate predictions than those assuming no
24 such increases (best-performing VE setting: 90/95% vs. 30/67% baseline for the 1st/2nd dose).
25 Counterfactual modeling indicates that high vaccination coverage for 1st vaccine-dose in India
26 (~50% by mid-Oct 2021) combined with the boosting of VE among recoverees averted around
27 60% of infections during July – mid-Oct 2021.

28

29 **Interpretation:** Non-pharmaceutical interventions, infection seasonality, and high coverage of
30 1-dose vaccination likely all contributed to pandemic dynamics in India during 2021. Given the
31 shortage of COVID-19 vaccines globally and boosting of VE, for populations with high prior
32 infection rates, prioritizing the first vaccine-dose may protect more people.

33

34 **Key words:** COVID-19; Delta SARS-CoV-2 variant; India; vaccination effectiveness; boosting;
35 prior infection

36

37 Research in context

38 Evidence before this study

39 We searched PubMed for studies published through Nov 3, 2021 on the Delta (B.1.617.2) SARS-
40 CoV-2 variant that focused on three areas: 1) transmissibility [search terms: (“Delta variant” OR
41 “B.1.617”) AND (“transmission rate” OR “growth rate” OR “secondary attack rate” OR
42 “transmissibility”)]; 2) immune response ([search terms: (“Delta variant” OR “B.1.617”) AND
43 (“immune evas” OR “immune escape”)]; and 3) vaccine effectiveness ([search terms: (“Delta
44 variant” OR “B.1.617”) AND (“vaccine effectiveness” OR “vaccine efficacy” OR “vaccination”)].
45 Our search returned 256 papers, from which we read the abstracts and identified 54 relevant
46 studies.

47

48 Forty-two studies addressed immune evasion and/or vaccine effectiveness. Around half (n=19)
49 of these studies measured the neutralizing ability of convalescent sera and/or vaccine sera
50 against Delta and most reported some reduction (around 2- to 8-fold) compared to ancestral
51 variants. The remainder (n=23) used field observations (often with a test-negative or cohort-
52 design) and reported lower VE against infection but similar VE against hospitalization or death.
53 Together, these laboratory and field observations consistently indicate that Delta can evade
54 preexisting immunity. In addition, five studies reported higher B-cell and/or T-cell vaccine-
55 induced immune response among recovered vaccinees than naïve vaccinees, suggesting
56 potential boosting of pre-existing immunity; however, all studies were based on small samples
57 (n = 10 to 198 individuals).

58
59 Sixteen studies examined transmissibility, including 1) laboratory experiments (n=6) showing
60 that Delta has higher affinity to the cell receptor, fuses membranes more efficiently, and/or
61 replicates faster than other SARS-CoV-2 variants, providing biological mechanisms for its higher
62 transmissibility; 2) field studies (n=5) showing higher rates of breakthrough infections by Delta
63 and/or higher viral load among Delta infections than other variants; and 3) modeling/mixed
64 studies (n=5) using genomic or case data to estimate the growth rate or reproduction number,
65 reporting a 60-120% increase. Only one study jointly estimated the increase in transmissibility
66 (1.3-1.7-fold, 50% CI) and immune evasion (10-50%, 50% CI); this study also reported a 27.5%
67 (25/91) reinfection rate by Delta.

68
69 **Added value of this study**

70 We utilize observed pandemic dynamics and the differential vaccination coverage for two
71 vaccine doses in India, where the Delta variant was first identified, to estimate the
72 epidemiological properties of Delta and examine the impact of prior non-Delta infection on
73 immune boosting at the population level. We estimate that Delta variant can escape immunity
74 from prior wildtype infection roughly one-third of the time and is around 60% more infectious
75 than wildtype SARS-CoV-2. In addition, our analysis suggests the large increase in population
76 receiving their first vaccine dose (~50% by end of Oct 2021) combined with the boosting effect
77 of vaccination for non-Delta infection recoverees likely mitigated epidemic intensity in India
78 during July – Oct 2021.

79
80 **Implications of all the available evidence**

81 Our analysis reconstructs the interplay and effects of non-pharmaceutical interventions,
82 infection seasonality, Delta variant emergence, and vaccination on COVID-19 pandemic
83 dynamics in India. Modeling findings support prioritizing the first vaccine dose in populations
84 with high prior infection rates, given vaccine shortages.

85
86

87 **INTRODUCTION**

88 The Delta (PANGO lineage: B.1.617.2) SARS-CoV-2 variant of concern (VOC)¹⁻⁴ has spread
89 quickly to over 170 countries (GISAID,⁵ as of 11/3/2021). Several lines of evidence have
90 indicated that Delta is able to evade immunity from prior infection by preexisting variants;
91 these include reduced neutralizing ability of convalescent sera and vaccinee sera against
92 Delta,⁶⁻⁹ reduced vaccine effectiveness (VE) against infection,¹⁰⁻¹³ and reduced VE against
93 symptomatic disease after 1-dose of vaccine (but only slight reduction for full vaccination).¹⁴⁻¹⁶
94 In addition, studies have found a higher secondary attack rate, growth rate, or reproduction
95 number for Delta than prior variants including Alpha (range of the mean estimates: 60-
96 120%).^{2,17-21} In particular, a recent study, fitting a model to mortality data in Delhi, India,
97 estimated a 1.3-1.7-fold (50% CI) increase in transmissibility and 10-50% (50% CI) immune
98 evasion for Delta; however, the authors noted large uncertainty in their estimates.²² Further,
99 factors such as host behavioral changes and seasonal modulation of risk due to changes in
100 environmental conditions are difficult to account for and could confound these estimates. As a
101 result, estimates of prior immunity evasion and relative transmissibility for Delta and the
102 contributions of these properties to the rapid spread of this variant remain uncertain.

103

104 India, where Delta was first identified, experienced an intensive pandemic wave in late March
105 2021. However, unlike many places seeing a prolonged Delta pandemic wave, the Delta wave in
106 India only lasted 3 months and declined rapidly after peaking mid-May. Since June 2021 cases
107 have remained low. A high infection rate after the Delta wave has been cited as a reason for
108 this dramatic epidemic decline, as vaccination coverage was low at the time (4.2% fully
109 vaccinated at the end of June 2021). However, given an estimated basic reproduction number
110 (R_0) of 6-7,²⁰ roughly 83-86% ($1 - 1/R_0$) of the population would need immunity for the Delta
111 epidemic to subside. Assuming 10-50% immunity escape²² and a 25-35% infection rate prior to
112 the Delta wave,²³ this implies that 53-73% of India's 1.4 billion people would have been infected
113 by Delta within the span of 3 months, despite a national lockdown at the time.

114

115 To better understand COVID-19 pandemic dynamics in India and the epidemiological
116 characteristics of Delta, here we utilize a model-inference method recently developed for SARS-
117 CoV-2 VOCs. The model-inference method incorporates epidemiological, population mobility,
118 and weather data to model SARS-CoV-2 transmission dynamics, while accounting for case
119 under-ascertainment, impacts of non-pharmaceutical interventions (NPIs) and vaccination,
120 infection seasonality, and new variants.²⁴ Applying this method, we have jointly estimated the
121 immune escape potential and change in transmissibility for Alpha, Beta, and Gamma,
122 separately, using data from countries where these three VOCs were first reported.²⁴ In
123 addition, several laboratory studies have reported stronger vaccine-induced immune responses
124 among recovered vaccinees than naïve vaccinees, suggesting potential boosting of pre-existing
125 immunity. In India, while only 23% of the population have received two vaccine doses, 53%
126 have received their first vaccine dose, as of the end of Oct 2021. This large discrepancy in one-
127 and two dose coverage, combined with a likely high population infection rate, offers an
128 opportunity to examine the boosting effect of prior non-Delta infection on vaccine-induced
129 immunity at the population level. Therefore, in this study, we first reconstruct the pandemic
130 dynamics in India during March 2020 – June 2021 and estimate key epidemiological
131 characteristics of Delta. We then further use our model estimates to retrospectively predict
132 cases and deaths during July – Oct 2021, under various vaccination and VE scenarios, and
133 compare these simulations to observations in order to estimate the impact of vaccination and
134 VE for those with prior non-Delta infection.

135

136 **METHODS**

137 **Data sources and processing**

138 We used reported COVID-19 case and mortality data to capture transmission dynamics,
139 weather data to estimate infection seasonality, mobility data to represent concurrent NPIs, and
140 vaccination data to account for changes in population susceptibility due to vaccination in the
141 model-inference system. COVID-19 case and mortality data from the week of March 8, 2020
142 (the first week COVID-19 deaths were reported in India) to the week of Oct 17, 2021 came from
143 the COVID-19 Data Repository of the Center for Systems Science and Engineering (CSSE) at

144 Johns Hopkins University.^{25,26} Surface station temperature and humidity data were accessed
145 using the “rnoaa” R package.²⁷ We then aggregated these data for all weather stations in India
146 (n = 390 stations) with measurements from Jan 2020 to Oct 2021 and calculated the average for
147 each week of the year. Mobility data were derived from Google Community Mobility Reports;²⁸
148 we aggregated all business-related categories (i.e., retail and recreational, transit stations, and
149 workplaces) in all locations in India to weekly intervals. Vaccination data (1st and 2nd dose) were
150 obtained from Our World in Data.^{29,30}

151

152 **Model-inference system**

153 The model-inference system was developed and described in detail in our previous study.³¹

154 Below we describe each component in brief.

155

156 *Epidemic model*

157 The epidemic model follows an SEIRSV (susceptible-exposed-infectious-recovered-susceptible-
158 vaccination) construct per Eqn 1:

$$\left\{ \begin{array}{l} \frac{dS}{dt} = \frac{R}{L_t} - \frac{b_t e_t m_t \beta_t IS}{N} - \varepsilon - v_{1,t} - v_{2,t} \\ \frac{dE}{dt} = \frac{b_t e_t m_t \beta_t IS}{N} - \frac{E}{Z_t} + \varepsilon \\ \frac{dI}{dt} = \frac{E}{Z_t} - \frac{I}{D_t} \\ \frac{dR}{dt} = \frac{I}{D_t} - \frac{R}{L_t} + v_{1,t} + v_{2,t} \end{array} \right.$$

159

160 where S , E , I , R are the number of susceptible, exposed (but not yet infectious), infectious, and
161 recovered/immune/deceased individuals; N is the population size; and ε is the number of
162 travel-imported infections. In addition, the model includes the following key components:

163 1) Virus-specific properties, including the time-varying variant-specific transmission rate
164 β_t , latency period Z_t , infectious period D_t , and immunity period L_t . Note the subscript, t , denotes
165 time in week, as all parameters are estimated for each week as described below.

166 2) The impact of NPIs. Specifically, we use relative population mobility (see data above)
167 to adjust the transmission rate via the term m_t . To further account for potential changes in
168 effectiveness, the model additionally includes a parameter, e_t , to scale NPI effectiveness.

169 3) The impact of vaccination, via the terms $v_{1,t}$ and $v_{2,t}$. Specifically, $v_{1,t}$ is the number of
170 individuals successfully immunized after the first dose of vaccine and is computed using
171 vaccination data and vaccine efficacy for 1st dose; and $v_{2,t}$ is the additional number of
172 individuals successfully immunized after the second vaccine dose (i.e., excluding those
173 successfully immunized after the first dose).

174 4) Infection seasonality, computed using temperature and specific humidity data as
175 described previously (see supplemental material of Yang and Shaman²⁴). The estimated relative
176 seasonal trend, b_t , is used to adjust the relative transmission rate at time t .

177

178 *Observation model to account for under-detection and delay*

179 Using the model-simulated number of infections occurring each day, we further computed the
180 number of cases and deaths each week to match with the observations, as done in Yang et al.³²
181 For example, for case data, we include 1) a time-lag from infectiousness to detection (i.e., an
182 infection being diagnosed as a case) to account for delays in detection; and 2) an infection-
183 detection rate (r_t), i.e. the fraction of infections (including subclinical or asymptomatic
184 infections) reported as cases, to account for under-detection. To compute the model-simulated
185 number of new cases per week, we multiply the model-simulated number of new infections per
186 day by the infection-detection rate, and further distribute these simulated cases in time per the
187 distribution of time-from-infectiousness-to-detection. We then aggregate the daily lagged,
188 simulated cases to weekly totals for model inference (see below).

189

190 *Model inference and parameter estimation*

191 The inference system uses the EAKF,³³ a Bayesian statistical method, to estimate model state
192 variables (i.e., S, E, I, R from Eqn 1) and parameters (i.e., $\beta_t, Z_t, D_t, L_t, e_t$, from Eqn 1 as well as r_t
193 and other parameters from the observation model). Briefly, the EAKF uses an ensemble of
194 model realizations ($n=500$ here), each with initial parameters and variables randomly drawn

195 from a *prior* range (see Table S1). After model initialization, the system integrates the model
196 ensemble forward in time for a week (per Eqn 1) to compute the prior distribution for each
197 model state variable and parameter, as well as the model-simulated number of cases and
198 deaths for that week. The system then combines the prior estimates with the observed case
199 and death data for the same week to compute the posterior per Bayes' theorem.³³ During this
200 filtering process, the system updates the posterior distribution of all model variables and
201 parameters for each week.

202

203 *Estimating the immune escape potential and changes in transmissibility for Delta*

204 To identify the most plausible combination of changes in transmissibility and level of immune
205 evasion, per methods developed in ref²⁴, we ran the model-inference, repeatedly and in turn,
206 to test 14 major combinations of these two quantities and select the best performing run.
207 Based on the best-performing model estimates, we then computed the variant-specific
208 transmissibility as the product of the variant-specific transmission rate (β_t) and infectious
209 period (D_t). To reduce uncertainty, we averaged transmissibility estimates over the first
210 pandemic wave and the period when Delta is dominant, separately. We then computed the
211 average change in transmissibility due to Delta as the ratio of the two averaged estimates (i.e.,
212 after: before the rise of Delta). To quantify immune evasion, we recorded the changes in
213 susceptibility over time and then computed the level of immune evasion as the ratio of the
214 total increase in susceptibility due to immune evasion during the second wave to the model-
215 estimated population immunity at the end of the first wave.

216

217 To account for model stochasticity, we repeated the model-inference process 300 times, each
218 with 500 model realizations and summarized the results from all 150,000 model estimates. As a
219 sensitivity test and part of the effort to examine the impact of prior non-Delta infection on VE,
220 we performed the analysis using 12 different VE settings (see details below).

221

222 **Model validation using independent data**

223 To compare model estimates with independent observations not assimilated into the model-
224 inference system, we identified three measurements of cumulative infection rates from three
225 nationwide serology surveys in India: i) the first national serosurvey conducted during May 11 –
226 June 4, 2020 (n = 28,000 adults 18 years or older);³⁴ ii) the second national serosurvey
227 conducted during August 18 – September 20, 2020 (n = 29,082 individuals 10 years or older);³⁵
228 and iii) the third national serosurvey conducted during December 18, 2020 – January 6, 2021 (n
229 = 28,598 individuals 10 years or older).³⁶ To account for the delay in antibody generation, we
230 shifted the timing of each serosurvey 14 days when comparing survey results to model-
231 inference system estimates of cumulative infection rates in Fig 1B.

232

233 **Estimating the impact of vaccination and prior non-Delta infection on boosting vaccine-** 234 **induced immunity**

235 We generated retrospective projections of cases and deaths from the week starting 7/4/2021
236 to the week starting 10/17/2021 (i.e., 16 weeks following the model-inference period), under
237 various vaccination and VE settings. We considered four levels of VE for those recovered from
238 non-Delta infection: 1) No boosting effect, i.e., using the same VE values as those without prior
239 infection. Here, we set VE at fourteen days after the 1st dose (VE1) to 30% and at seven days
240 after the 2nd dose (VE2) to 67%, based on data for the AstraZeneca vaccine against Delta;¹⁵ 2)
241 Higher VE for the 1st dose but no future boosting for the 2nd dose (here, VE1 is set to 40%, 50%,
242 or 60%, and VE2 fixed at 67%); 3) Higher VE for the 2nd dose but not 1st dose (here, VE1 is fixed
243 at 30% and VE2 set to 75%, 85%, or 95%); and 4) Higher VE for both doses (here, VE1/VE2 are
244 set to 50%/75%, 60%/80%, 70%/85%, 80%/90%, or 90%/95%). To test the impact of
245 vaccination, in addition to projections using reported vaccination rates, we also generated
246 counterfactual projections assuming no further vaccination during the 16-week period.

247

248 For all projections, the model was initiated using model-inference estimates made at the week
249 of 6/27/2021, except for the infection-fatality risk (IFR). For IFR, estimates were decreasing
250 during June 2020 (Fig S1B) and model-inference extended to the end of July 2021 showed
251 continued decreases, likely due to improved healthcare and increased protection from prior

252 infection or vaccination. We thus assumed that IFR would decrease linearly for the first 6 weeks
253 of the projection period and then flatten and remain at that low IFR until the week of
254 10/17/2021. To account for NPIs, we used mobility data during the week of 7/4/2021 – the
255 week of 10/17/2021. As for the model-inference runs, we repeated the projections for each
256 scenario 300 times (each with 500 model realizations) and summarized the projections from all
257 runs. To evaluate the projection accuracy, we computed the relative root-mean-square-error
258 (RRMSE) and correlation between the projected and observed values for cases and deaths,
259 respectively.

260

261 **RESULTS**

262 **The first COVID-19 pandemic wave in India, March 2020 – January 2021**

263 From March 2020 to January 2021 India recorded over 10 million COVID-19 cases (0.77% of its
264 population); however, a nationwide serology survey suggested that ~24% of its population had
265 been infected by December 2020.²³ Accounting for under-detection of infection (Fig S1),
266 implemented non-pharmaceutical interventions (NPIs), seasonality, and vaccination, we used
267 the model-inference system to reconstruct pandemic dynamics in India since March 2020 (Fig
268 1A). Model-estimated infection rates closely match with measurements from three nationwide
269 serologic surveys conducted during the early, mid, and late phases of the first pandemic wave
270 (Fig 1B). Our analysis indicates that the 2-month long national lockdown (March 24 – May 31,
271 2020) and the less favorable weather conditions during pre-monsoon season (i.e., March –
272 May) likely contributed to initial low infection rates. By mid-May 2020, the model-inference
273 system estimates that only 0.43% (95% CrI: 0.19 – 1.7%) of the population had been infected
274 [vs. 0.73% (95% CI: 0.34%, 1.13%) among adults estimated by serosurvey³⁴]. As the country
275 lifted its lockdown in June 2020 and entered the monsoon season (June – September), when
276 conditions are likely more favorable for transmission (Fig 1C), the first pandemic wave began.
277 Nevertheless, continued regional restrictions during June – November 2020 and less favorable
278 weather conditions during the autumn (October – November; see mobility and seasonal trends
279 in Fig 1C) likely mitigated pandemic intensity. The estimated mean of the reproduction number
280 R_t (i.e., average number of secondary infections per primary infection) was above 1 but less

281 than 1.35 from June to mid-September; in addition, R_t dropped below 1 during October –
282 November (Fig 1D). By the end of January 2021 when case rates reached a minimum following
283 the first wave, the model-inference system estimates that 26.1% (95% CrI: 19.9 – 33.0%) of the
284 population had been infected (Fig 1B).

285

286 **The second pandemic wave in India and estimated epidemiological characteristics of Delta**

287 Infections resurged dramatically in late March 2021, largely due to the rise of the Delta variant.
288 Despite a weeks-long second national lockdown implemented beginning April 20, 2021, India
289 reported another 19 million cases during late March – June 2021, about twice the number
290 reported during the previous 12 months. Accounting for under-detection (Fig S1), we estimate
291 that 32.3% (95% CrI: 22.4 – 46.5%) of the population were infected during this 3-month period,
292 including reinfections. This intense transmission was likely facilitated by the higher
293 transmissibility and immune evasive capabilities of the Delta variant. Estimated transmissibility
294 increased substantially during the second pandemic wave (Fig 1E). In addition, estimated
295 population susceptibility increased at the start of the second pandemic wave (Fig 1F),
296 suggesting loss of population immunity against Delta. Due to this immune escape, an estimated
297 50.5% (95% CrI: 21.8 – 79.0%) of the population remained susceptible at the end of June 2021,
298 despite two large pandemic waves and rollout of mass vaccination (of note, 19% of the
299 population had received at least 1 dose of vaccine by the end of June 2021). These findings
300 along with the seasonal trends described above suggest that the decline of the second wave
301 was largely due to the NPIs implemented and less favorable weather conditions during March –
302 May, rather than high population immunity.

303

304 Combining the model-inference estimates during the first and second pandemic waves in India,
305 we estimated that Delta was able to escape immunity among 34.6% (95% CI: 0 – 64.2%) of
306 individuals with prior wildtype infection and was 57.0% (95% CI: 37.9 – 75.6%) more
307 transmissible than wildtype SARS-CoV-2. Estimates are similar under different VE settings (Fig
308 S2).

309

310 **Impact of vaccination and prior non-Delta infection on boosting vaccine-induced immunity**

311 Despite the likely conducive conditions during the monsoon season (June – September), easing
312 of NPIs, and relatively high susceptibility estimated at the end of June 2021, cases and deaths in
313 India remained at relatively low levels during July – Oct 2021. Counterfactual modeling suggests
314 that the faster rollout of vaccination during this period substantially mitigated the epidemic risk
315 (Fig 2). Projected cases and deaths assuming no further vaccination uptake are much higher
316 than observed; In contrast, models including the reported vaccination rates more closely match
317 reported cases and deaths (Fig 2). Further, models assuming higher VE for non-Delta infection
318 recoverees generated more accurate projections than those assuming no boosting effect (Fig
319 3). The boosting effect appears to be more pronounced for the 1st vaccine dose (see, e.g., Fig 3A
320 where larger dots, representing higher VE after the 1st dose, had smaller errors). Overall, the
321 model assuming 90%/95% VE for the 1st/2nd dose of vaccine for non-Delta infection recoverees
322 generated the most accurate projections. These projections estimate that vaccination rollout
323 combined with the boosting effect averted 57% of infections during July – mid-Oct 2021.

324

325 **Discussion**

326 Combining epidemiological, behavioral, and weather observational data with a comprehensive
327 model-inference system, we estimate the Delta SARS-CoV-2 variant escaped immunity in
328 roughly one-third of individuals with wildtype infection during the previous year and was
329 around 60% more infectious than wildtype SARS-CoV-2. In addition, our analysis suggests the
330 large increase in population receiving their first vaccine dose (~50% by end of Oct 2021)
331 combined with the boosted VE for non-Delta infection recoverees likely mitigated the epidemic
332 intensity in India in recent months.

333

334 Previously, we have estimated the changes in transmissibility and immune escape potential for
335 three other major SARS-CoV-2 VOCs: namely, a 46.6% (95% CI: 32.3 – 54.6%) increase in
336 transmissibility but nominal immune escape for Alpha (i.e., B.1.1.7), a 32.4% (95% CI: 14.6 –
337 48.0%) increase in transmissibility and 61.3% (95% CI: 42.6 – 85.8%) immune escape for Beta
338 (i.e., B.1.351), and a 43.3% (95% CI: 30.3 – 65.3%) increase in transmissibility and 52.5% (95%

339 CI: 0 – 75.8%) immune escape for Gamma (i.e., P.1). Compared with Alpha, data from the UK
340 have shown that the secondary attack rate for contacts of cases with Delta was around 1.5
341 times higher than Alpha (12.4% vs. 8.2%), during March 29 – May 11, 2021.² In a partially
342 immunized population, the secondary attack rate reflects the combined outcome of the
343 transmissibility of the etiologic agent and population susceptibility to that agent. Consistent
344 with the UK data, our estimates of the relative transmissibility and immune escape potential
345 combine to a 44.1% (95% CI: 4.2 – 86.6%) higher secondary attack rate by Delta than Alpha [i.e.,
346 $(1+57\%)/(1+46.6\%) \times (1+34.6\%) - 1 = 44.1\%$ increase]. This higher competitiveness of Delta
347 over Alpha explains the rapid variant displacement observed in regions previously dominated
348 by Alpha (e.g. the UK and the US).

349
350 In addition, we estimate that 34.6% (95% CI: 0 – 64.2%) of individuals with acquired immunity
351 from wildtype infection would be susceptible to Delta due to immune escape. This estimate is
352 also in line with a recent study²² reporting a 27.5% reinfection rate during the Delta pandemic
353 wave in Delhi, India, based on a small subset of people with repeated serology measures. In
354 addition to immune escape from wildtype infection, studies have also reported reduced ability
355 of sera from Beta- and Gamma-infection recoverees to neutralize Delta,^{8,37} suggesting Delta can
356 also escape immunity conferred by those two VOCs. Such immune escape ability would also
357 allow Delta to rapidly replace Beta and Gamma in regions previously hard-hit by those two
358 VOCs, as has been observed in many countries in Africa and South America.⁵ More
359 fundamentally, these findings highlight the complex, non-linear immune landscape of SARS-
360 CoV-2 and the importance to monitor the immune escape potential of new variants against
361 both previous and concurrent circulating variants.

362
363 Despite the successful development of multiple vaccines, shortage of supplies – particularly in
364 resource-limited countries – remains an impediment to global mass vaccination.³⁸ In response,
365 researchers have proposed dose sparing strategies such as fractionation³⁹ and 1-dose
366 vaccination for recoverees.⁴⁰ The latter 1-dose strategy draws on laboratory studies showing
367 higher vaccine-induced immune response among recovered vaccinees than naïve vaccinees

368 (i.e., boosting of pre-existing immunity).⁴¹⁻⁴⁴ Here, we utilized model-inference estimates and
369 vaccination data in India to test the impact of boosting at the population level. The findings
370 further support the effectiveness of 1-dose vaccination for recoverees. In light of continued
371 vaccine shortages, prioritizing first-dose vaccination thus may be an effective strategy for
372 mitigating COVID-19 burden in countries with high underlying SARS-CoV-2 infection rates.
373
374 Due to a lack of detailed epidemiological data (e.g., age-specific and subnational) and thus
375 model simplification, our estimates have uncertainties as indicated by the large credible
376 intervals. Nevertheless, these estimates are in line with independent data from three
377 nationwide serology surveys conducted at three time points during the first pandemic wave in
378 India (Fig 1B), as well as Delta-related epidemiological data from the UK² and Delhi, India,²² as
379 discussed above; these consistencies support the accuracy of our estimates. Unlike estimates
380 from the contact tracing data, however, here we are able to separately quantify the changes in
381 transmissibility and immune escape potential of the Delta variant. In addition, our analysis also
382 suggests high 1-dose vaccine effectiveness among those with prior infection. These findings
383 and the methods used to generate them could support better understanding of future SARS-
384 CoV-2 variant dynamics given local prior infection rates, variant prevalence, and vaccination
385 coverage.

386
387 **Data Availability:** All data used in this study are publicly available as described in the “Data
388 sources and processing” section.

389
390 **Code availability:** All source code and data necessary for the replication of our results and
391 figures are made publicly available at https://github.com/wan-yang/covid_voc_delta.

392
393 **Acknowledgements:** This study was supported by the National Institute of Allergy and
394 Infectious Diseases (AI145883 and AI163023), the National Science Foundation Rapid Response
395 Research Program (RAPID; DMS-2027369) and a gift from the Morris-Singer Foundation.

396

397 **Author contributions:** WY designed the study, performed the analysis, and wrote the first draft;
398 JS provided input to the analysis and contributed to the final draft.

399

400 **Competing interests:** JS and Columbia University disclose partial ownership of SK Analytics. JS
401 discloses consulting for BNI.

402 **References:**

- 403 1. World Health Organization. Tracking SARS-CoV-2 variants. 2021.
404 <https://www.who.int/en/activities/tracking-SARS-CoV-2-variants/>.
- 405 2. Public Health England. SARS-CoV-2 variants of concern and variants under investigation in
406 England. Technical briefing 14. 2021.
407 [https://assets.publishing.service.gov.uk/government/uploads/system/uploads/attachmen](https://assets.publishing.service.gov.uk/government/uploads/system/uploads/attachment_t_data/file/991343/Variants_of_Concern_VOC_Technical_Briefing_14.pdf)
408 [t_data/file/991343/Variants of Concern VOC Technical Briefing 14.pdf](https://assets.publishing.service.gov.uk/government/uploads/system/uploads/attachment_t_data/file/991343/Variants_of_Concern_VOC_Technical_Briefing_14.pdf) (accessed
409 6/16/2021 2021).
- 410 3. National Collaborating Centre for Infectious Diseases. Updates on COVID-19 Variants of
411 Concern. 4/26/2021 2021. <https://nccid.ca/covid-19-variants/> (accessed 5/3/2021 2021).
- 412 4. Centers for Disease Control and Prevention. SARS-CoV-2 Variant Classifications and
413 Definitions. 2021. <https://www.cdc.gov/coronavirus/2019-ncov/variants/variant-info.html>
414 (accessed 6/17/2021 2021).
- 415 5. Global Initiative on Sharing All Influenza Data (GISAID). Tracking of Variants. 6/16/2021
416 2021. <https://www.gisaid.org/hcov19-variants/> (accessed 6/16/2021 2021).
- 417 6. Mlcochova P, Kemp SA, Dhar MS, et al. SARS-CoV-2 B.1.617.2 Delta variant replication and
418 immune evasion. *Nature* 2021.
- 419 7. Wall EC, Wu M, Harvey R, et al. Neutralising antibody activity against SARS-CoV-2 VOCs
420 B.1.617.2 and B.1.351 by BNT162b2 vaccination. *Lancet* 2021.
- 421 8. Liu C, Ginn HM, Dejnirattisai W, et al. Reduced neutralization of SARS-CoV-2 B.1.617 by
422 vaccine and convalescent serum. *Cell* 2021; **184**(16): 4220-+.

- 423 9. Arora P, Sidarovich A, Krüger N, et al. B.1.617.2 enters and fuses lung cells with increased
424 efficiency and evades antibodies induced by infection and vaccination. *Cell Reports* 2021;
425 **37**(2): 109825.
- 426 10. Chemaitelly H, Tang P, Hasan MR, et al. Waning of BNT162b2 Vaccine Protection against
427 SARS-CoV-2 Infection in Qatar. *N Engl J Med* 2021.
- 428 11. Goldberg Y, Mandel M, Bar-On YM, et al. Waning Immunity after the BNT162b2 Vaccine in
429 Israel. *N Engl J Med* 2021.
- 430 12. Puranik A, Lenehan PJ, Silvert E, et al. Comparison of two highly-effective mRNA vaccines
431 for COVID-19 during periods of Alpha and Delta variant prevalence. *medRxiv* 2021:
432 2021.08.06.21261707.
- 433 13. Elliott P, Haw D, Wang H, et al. Exponential growth, high prevalence of SARS-CoV-2, and
434 vaccine effectiveness associated with the Delta variant. *Science* 2021: eabl9551.
- 435 14. Bernal JL, Andrews N, Gower C, et al. Effectiveness of COVID-19 vaccines against the
436 B.1.617.2 variant. *medRxiv* 2021: 2021.05.22.21257658.
- 437 15. Bernal JL, Andrews N, Gower C, et al. Effectiveness of Covid-19 Vaccines against the
438 B.1.617.2 (Delta) Variant. *New England Journal of Medicine* 2021; **385**(7): 585-94.
- 439 16. Seppala E, Veneti L, Starrfelt J, et al. Vaccine effectiveness against infection with the Delta
440 (B.1.617.2) variant, Norway, April to August 2021. *Eurosurveillance* 2021; **26**(35).
- 441 17. Allen H, Vusirikala A, Flannagan J, et al. Household transmission of COVID-19 cases
442 associated with SARS-CoV-2 delta variant (B.1.617.2): national case-control study. *The*
443 *Lancet regional health Europe* 2021: 100252.
- 444 18. Challen R, Dyson L, Overton CE, et al. Early epidemiological signatures of novel SARS-CoV-
445 2 variants: establishment of B.1.617.2 in England. *medRxiv* 2021: 2021.06.05.21258365.
- 446 19. Earnest R, Uddin R, Matluk N, et al. Comparative transmissibility of SARS-CoV-2 variants
447 Delta and Alpha in New England, USA. *medRxiv* 2021.
- 448 20. Vohringer HS, Sanderson T, Sinnott M, et al. Genomic reconstruction of the SARS-CoV-2
449 epidemic in England. *Nature* 2021.
- 450 21. Campbell F, Archer B, Laurenson-Schafer H, et al. Increased transmissibility and global
451 spread of SARS-CoV-2 variants of concern as at June 2021. *Eurosurveillance* 2021; **26**(24).

- 452 22. Dhar MS, Marwal R, Vs R, et al. Genomic characterization and epidemiology of an
453 emerging SARS-CoV-2 variant in Delhi, India. *Science* 2021: eabj9932.
- 454 23. Murhekar MV, Bhatnagar T, Thangaraj JWV, et al. SARS-CoV-2 seroprevalence among the
455 general population and healthcare workers in India, December 2020–January 2021. *Int J*
456 *Infect Dis* 2021; **108**: 145-55.
- 457 24. Yang W, Shaman J. Development of a model-inference system for estimating
458 epidemiological characteristics of SARS-CoV-2 variants of concern. *Nature*
459 *Communications* 2021; **12**: 5573.
- 460 25. COVID-19 Data Repository by the Center for Systems Science and Engineering (CSSE) at
461 Johns Hopkins University. 2021. <https://github.com/CSSEGISandData/COVID-19>.
- 462 26. Dong E, Du H, Gardner L. An interactive web-based dashboard to track COVID-19 in real
463 time. *Lancet Infect Dis* 2020; **20**(5): 533-4.
- 464 27. Chamberlain S, Anderson B, Salmon M, et al. Package ‘rnoaa’. 2021.
- 465 28. Google Inc. Community Mobility Reports. 2020.
466 <https://www.google.com/covid19/mobility/>.
- 467 29. Data on COVID-19 (coronavirus) vaccinations by Our World in Data. 2020.
468 <https://github.com/owid/covid-19-data/tree/master/public/data/vaccinations>.
- 469 30. Mathieu E, Ritchie H, Ortiz-Ospina E, et al. A global database of COVID-19 vaccinations.
470 *Nat Hum Behav* 2021; **5**(7): 947-53.
- 471 31. Yang W, Shaman J. Epidemiological characteristics of three SARS-CoV-2 variants of
472 concern and implications for future COVID-19 pandemic outcomes. *medRxiv* 2021:
473 2021.05.19.21257476.
- 474 32. Yang W, Kandula S, Huynh M, et al. Estimating the infection-fatality risk of SARS-CoV-2 in
475 New York City during the spring 2020 pandemic wave: a model-based analysis. *The Lancet*
476 *Infectious diseases* 2021; **21**(2): 203-12.
- 477 33. Anderson JL. An ensemble adjustment Kalman filter for data assimilation. *Mon Weather*
478 *Rev* 2001; **129**(12): 2884-903.

- 479 34. Murhekar MV, Bhatnagar T, Selvaraju S, et al. Prevalence of SARS-CoV-2 infection in India:
480 Findings from the national serosurvey, May-June 2020. *Indian J Med Res* 2020; **152**(1): 48-
481 57.
- 482 35. Murhekar MV, Bhatnagar T, Selvaraju S, et al. SARS-CoV-2 antibody seroprevalence in
483 India, August-September, 2020: findings from the second nationwide household
484 serosurvey. *The Lancet Global Health* 2021; **9**(3): e257-e66.
- 485 36. Murhekar MV, Bhatnagar T, Thangaraj JWV, et al. SARS-CoV-2 seroprevalence among the
486 general population and healthcare workers in India, December 2020 - January 2021. *Int J*
487 *Infect Dis* 2021; **108**: 145-55.
- 488 37. de Oliveira T, Lessells R. Update on Delta and other variants in South Africa and other
489 world. 2021. [https://www.krisp.org.za/manuscripts/DeltaGammaSummary_NGS-](https://www.krisp.org.za/manuscripts/DeltaGammaSummary_NGS-SA_6JulV2.pdf)
490 [SA_6JulV2.pdf](https://www.krisp.org.za/manuscripts/DeltaGammaSummary_NGS-SA_6JulV2.pdf).
- 491 38. Padma TV. COVID vaccines to reach poorest countries in 2023 — despite recent pledges.
492 7/5/2021 2021. <https://www.nature.com/articles/d41586-021-01762-w> (accessed
493 11/11/2021 2021).
- 494 39. Cowling BJ, Lim WW, Cobey S. Fractionation of COVID-19 vaccine doses could extend
495 limited supplies and reduce mortality. *Nature Medicine* 2021; **27**(8): 1321-3.
- 496 40. Sasikala M, Shashidhar J, Deepika G, et al. Immunological memory and neutralizing activity
497 to a single dose of COVID-19 vaccine in previously infected individuals. *International*
498 *Journal of Infectious Diseases* 2021; **108**: 183-6.
- 499 41. Andreano E, Paciello I, Piccini G, et al. Hybrid immunity improves B cells and antibodies
500 against SARS-CoV-2 variants. *Nature* 2021.
- 501 42. Lucas C, Vogels CBF, Yildirim I, et al. Impact of circulating SARS-CoV-2 variants on mRNA
502 vaccine-induced immunity. *Nature* 2021.
- 503 43. Sokal A, Barba-Spaeth G, Fernández I, et al. mRNA vaccination of naive and COVID-19-
504 recovered individuals elicits potent memory B cells that recognize SARS-CoV-2 variants.
505 *Immunity* 2021.

- 506 44. Sapkal GN, Yadav PD, Sahay RR, et al. Neutralization of Delta variant with sera of
507 Covishield™ vaccinees and COVID-19-recovered vaccinated individuals. *J Travel Med* 2021;
508 **28**(7).
509

Fig 1. Model-inference estimates and validation. (A) Model fit. (B) Model validation. (C) Observed relative mobility and estimated disease seasonal trend, compared to case and death rates over time. Key model-inference estimates are shown for the real-time reproduction number R_t (D), transmissibility (E), and population susceptibility (F). Blue lines and surrounding areas show the estimated mean, 50% (dark) and 95% (light) CrIs. Boxes and whiskers show the estimated mean, 50% and 95% CrIs for weekly cases and deaths in (A) and infection rates in (D) – (F). Grey shaded areas indicate the timing of national lockdowns (darker) or local restrictions (lighter); horizontal arrows indicate the timing of variant identification and vaccination rollout. In (C), for mobility (blue line; y-axis), values below 1 (dashed horizontal line) indicate reductions due to public health interventions. For the disease seasonal trend (orange line; y-axis), values above 1 indicate weather conditions more conducive for transmission than the yearly average and *vice versa*. *Note that the transmissibility estimates have removed the effects of changing population susceptibility, NPIs, and disease seasonality; thus, the trends are more stable than the reproduction number (R_t ; left column) and reflect changes in variant-specific properties.*

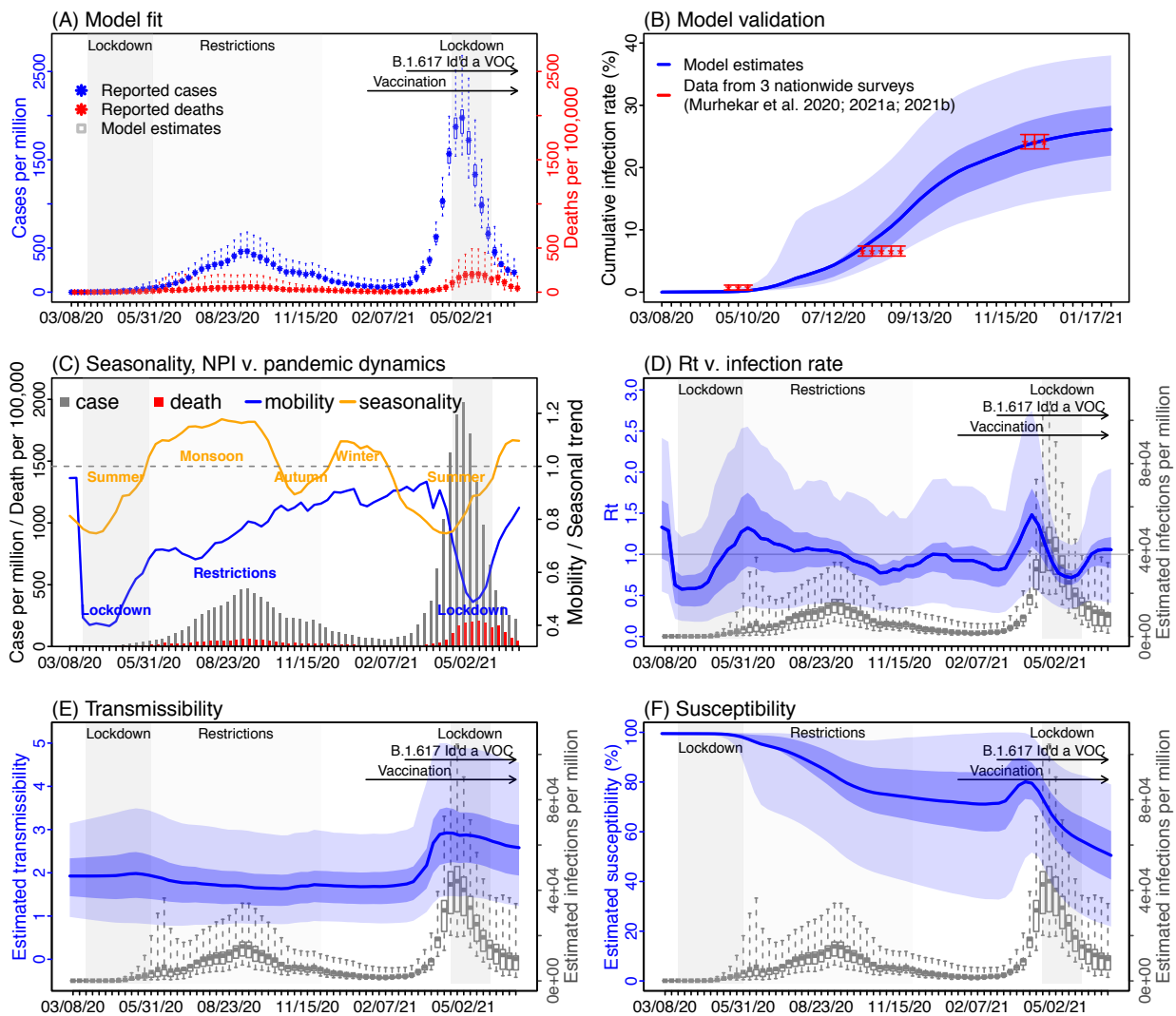


Fig 2. Impact of vaccination. Model projections of weekly number of reported cases (A) and reported deaths (B) for India during July – mid-Oct 2021, compared to reported data. Crosses ('x') show reported data (left y-axis). Red dashed lines show median counterfactual model projections assuming no further vaccination uptake during the 16-week period. Blue dashed lines show median model projections using reported vaccination rates and assuming 90%/95% vaccine effectiveness for individuals with prior non-Delta infection after the 1st/2nd vaccine dose. Shaded areas with the same color show projected interquartile ranges. For comparison, estimated seasonality (orange lines), reported mobility (dark-blue lines), and cumulative vaccination uptake (full bar for 1st dose and filled section for 2nd dose) are overlaid (see right y-axis scale). All numbers are scaled per one million people.

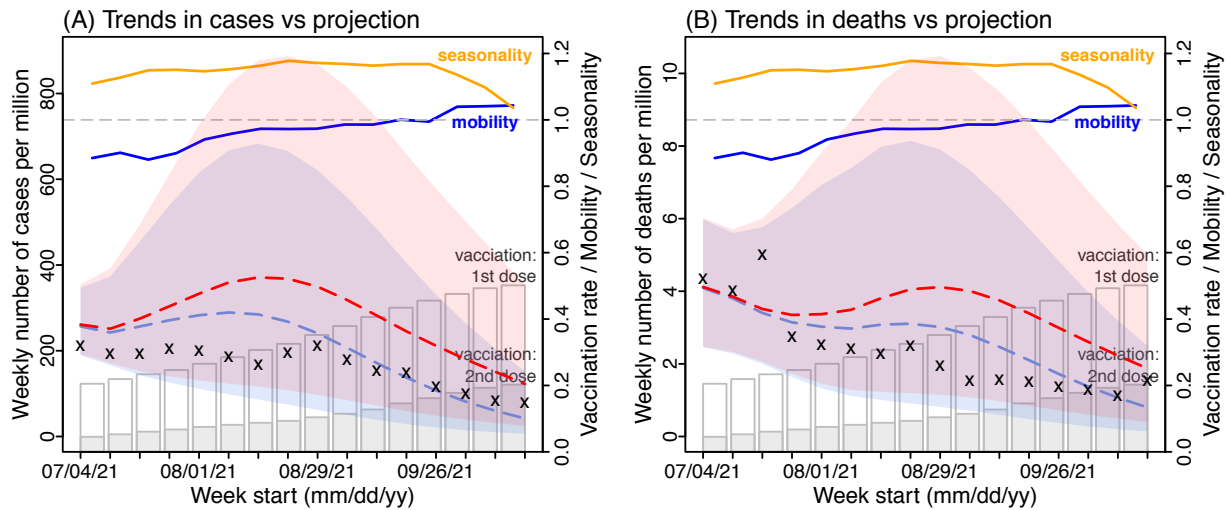
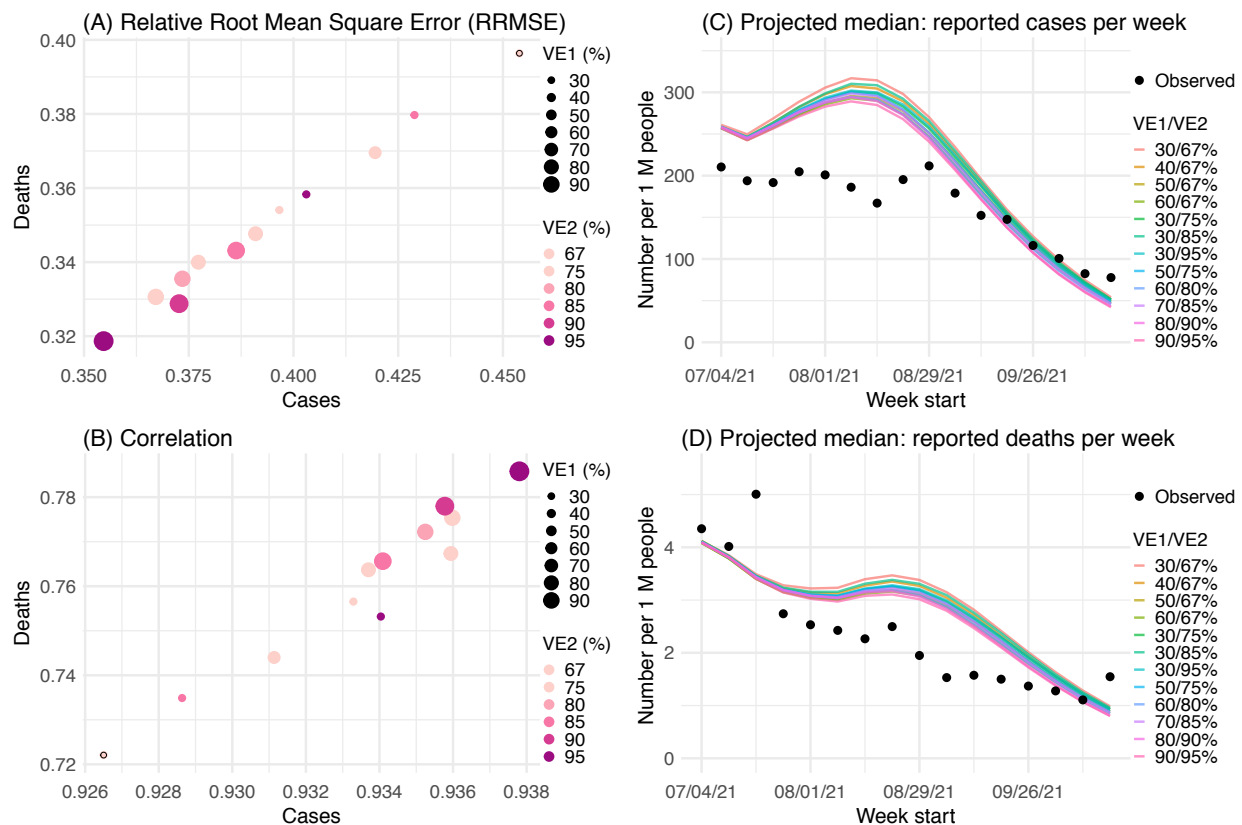


Fig 3. Impact of prior non-Delta infection on immune boosting. Model projections under different vaccine effectiveness (VE) settings are used to examine the most plausible VE for individuals with prior non-Delta infection, based on projection accuracy: (A) the relative root-mean-square-error (RRMSE) and (B) correlation between the projected and observed values for cases and deaths, respectively. The size of the dots represents VE for recoverees after the 1st vaccine dose and the color represents VE after the 2nd vaccine dose. The dots with the black circles represent the baseline VE setting (i.e. 30%/67% for the 1st/2nd dose). For comparison, projected weekly numbers of reported cases (C) and reported deaths (D) under different VE settings are plotted along with the weekly actuals. For clarity, only median projections are shown here; see example projections including interquartile ranges in Fig 2.



Supplemental Table and Figures

Table S1. Prior ranges for the parameters used in the model-inference system.

Parameter/ variable	Symbol	Prior range	Source/rationale
Initial exposed	$E(t=0)$	500 – 1000 times of the reported number of cases on the first week of simulation (i.e. the week of 3/8/2020)	Low infection-detection rate in first weeks.
Initial infectious	$I(t=0)$	Same as for $E(t=0)$	
Initial susceptible	$S(t=0)$	99 – 100% of the population	Almost everyone is susceptible initially
Population size	N	N/A	Based on data
Variant-specific transmission rate	β	[0.4, 0.7]	Based on R_0 estimates of around 1.5-4 for SARS-CoV-2. ¹⁻³ Slightly lower ranges are used here, as initial testing showed that use of higher values tended to overestimate the observations.
Scaling of effectiveness of NPI	e	[0.5, 1.5]	Around 1, with a large bound to be flexible.

Latency period	Z	[2, 5] days	Incubation period: 5.2 days (95% CI: 4.1, 7) ¹ ; latency period is likely shorter than the incubation period
Infectious period	D	[2, 5] days	Time from symptom onset to hospitalization: 3.8 days (95% CI: 0, 12.0) in China, ⁴ plus 1-2 days viral shedding before symptom onset. We did not distinguish symptomatic/asymptomatic infections.
Immunity period	L	[730, 1095] days	Assuming immunity lasts for 2-3 years
Mean of time from viral shedding to diagnosis	T_m	[5, 8] days	From a few days to a week from symptom onset to diagnosis/reporting, ⁴ plus 1-2 days of viral shedding (being infectious) before symptom onset. There may be a slightly longer delay for South Africa and Brazil.
Standard deviation (SD) of time from viral shedding to diagnosis	T_{sd}	[1, 3] days	To allow variation in time to diagnosis/reporting

Infection-detection rate	r	Starting from U[0.0001, 0.02] at time 0 and allowed to increase over time using space re-probing ⁵ with values drawn from U[0.015, 0.08] starting at week 8 (the week of 4/26/2020), U[0.02, 0.08] starting at week 15 (the week of 6/14/2020), U[0.01, 0.08] starting 1/17/2021 (around the end of the first pandemic wave), U[0.01, 0.05] starting 5/23/2021 (around the end of the Delta wave).	Large uncertainties; therefore, in general we use large prior bounds and large bounds for space re-probing (SR). Note that SR is only applied to 3-10% of the ensemble members and r can migrate outside either the initial range or the SR ranges during EAKF update. In India, due to the younger population age structure, infection detection rates were likely low throughout.
Infection fatality risk (IFR)		Starting from U[0.0001, 0.003] at time 0 and allowed to change over time using space re-probing ⁵ with values drawn from U[0.0001, 0.0015] starting at week 8 (the week of 4/26/2020), values drawn from U[0.0001, 0.0008] during the week of 7/05/2020 to the week of 3/21/2021 when case fatality risk was lower as computed from the data, values drawn from U[0.0001, 0.0015] starting the week of 4/4/2021 with the rise of Delta, values drawn from U[0.0001, 0.003] starting the week of 5/2/2021 when the healthcare systems began to be overwhelmed, and values drawn from U[0.0001, 0.0005] starting the week of 6/6/2021 when many have been infected or vaccinated and reported cases and deaths declined to low levels.	Based on previous estimates ⁶ but extend to have wider ranges. Note that SR is only applied to 3-10% of the ensemble members and IFR can migrate outside either the initial range or the SR ranges during EAKF update. In India, due to the younger population age structure, infection fatality risk was likely low throughout.
Vaccine efficacy (VE)		VE = 30% fourteen days after the 1 st dose, and 67% seven days after the 2 nd dose.	During 1/15/2021 – 6/27/2021, India used the Oxford/AstraZeneca and Covaxin vaccines; during 6/28/2021 – 10/31/2021,

Sputnik V was also used. Here we set the baseline VE based on data for the Oxford/AstraZeneca vaccine.⁷

References:

1. Li Q, Guan X, Wu P, et al. Early Transmission Dynamics in Wuhan, China, of Novel Coronavirus–Infected Pneumonia. *New Engl J Med* 2020.
2. Wu JT, Leung K, Leung GM. Nowcasting and forecasting the potential domestic and international spread of the 2019-nCoV outbreak originating in Wuhan, China: a modelling study. *Lancet* 2020; **395**(10225): 689-97.
3. Li R, Pei S, Chen B, et al. Substantial undocumented infection facilitates the rapid dissemination of novel coronavirus (SARS-CoV-2). *Science* 2020; **368**(6490): 489-93.
4. Zhang J, Litvinova M, Wang W, et al. Evolving epidemiology and transmission dynamics of coronavirus disease 2019 outside Hubei province, China: a descriptive and modelling study. *The Lancet Infectious diseases* 2020; **20**(7): 793-802.
5. Yang W, Shaman J. A simple modification for improving inference of non-linear dynamical systems. *arXiv* 2014: 1403.6804.
6. Verity R, Okell LC, Dorigatti I, et al. Estimates of the severity of coronavirus disease 2019: a model-based analysis. *The Lancet Infectious diseases* 2020; **20**(6): 669-77.
7. Bernal JL, Andrews N, Gower C, et al. Effectiveness of Covid-19 Vaccines against the B.1.617.2 (Delta) Variant. *New England Journal of Medicine* 2021; **385**(7): 585-94.

Fig S1. Estimated infection-detection rate (A) and infection-fatality risk (B) during each week of the study period. For comparison, estimated weekly infection rates are superimposed in each plot (right y-axis). Blue lines and surrounding areas show model estimated mean, 50% and 95% CrIs. Boxes and whiskers show model-estimated weekly infection rates (mean, 50% and 95% CrIs). Grey shaded boxes indicate the timing of lockdowns (darker) or local restrictions (lighter); horizontal arrows indicate the timing of variant identification and vaccination rollout. *Note that infection-fatality risk estimates were based on reported COVID-19 deaths and may not reflect the true values due to the likely under-reporting of COVID-19 deaths.*

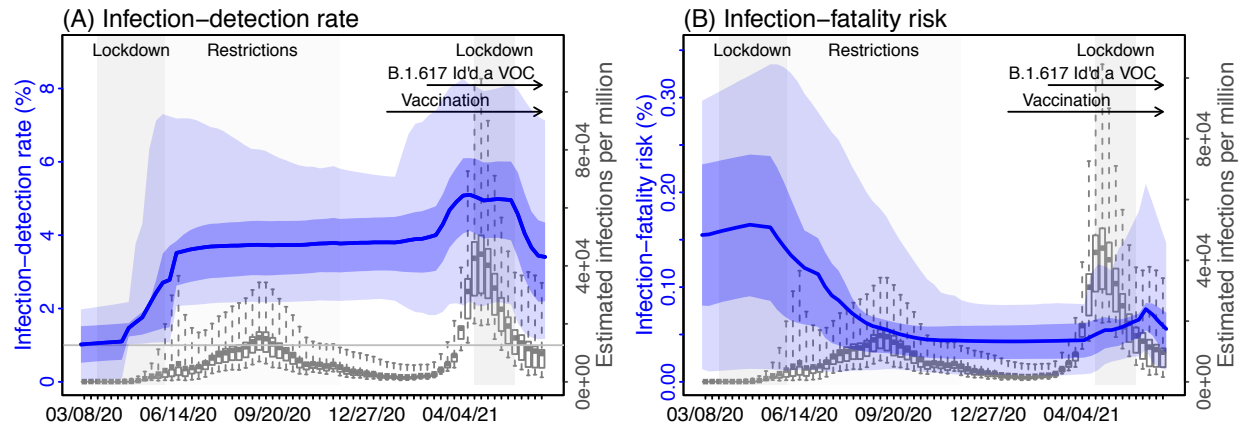


Fig S2. Estimated change in transmissibility and immune escape potential for the Delta variant, using different vaccine effectiveness (VE) settings for those with prior non-Delta infection. The baseline VE (i.e. 30%/67% for the 1st/2nd dose) was used for those without any prior infection; those infected by Delta were assumed to acquire immunity against this variant after recovery (see Eqn 1 in the main text). Twelve VE settings were tested (see x-axis label for VE after 1st/2nd dose). Model-inference was done 300 times (each with 500 ensemble members) for each VE setting. The boxplots summarize the distribution of estimates from the 300 runs: middle bar = median, edges = interquartile range, whiskers = 95% CI, red 'x' = mean.

